Amphiphilic Polymer Brush in a Mixture of Incompatible Liquids. Numerical Self-Consistent-Field Calculations

A. A. Mercurieva,[†] F. A. M. Leermakers,*[,‡] T. M. Birshtein,[†] G. J. Fleer,[‡] and E. B. Zhulina[†]

Institute of Macromolecular Compounds, Russian Academy of Sciences, 199004 St. Petersburg, Russia; and Laboratory of Physical Chemistry and Colloid Science, Wageningen University, Dreijenplein 6, 6703 HB Wageningen, The Netherlands

Received July 7, 1999; Revised Manuscript Received November 16, 1999

ABSTRACT: We studied a polymer brush composed of homodisperse end-grafted chains in a binary A−B solvent mixture by means of numerical self-consistent-field calculations. The focus is on the case that the solvents have a solubility gap in the bulk phase behavior, and we investigated the system near the bulk binodal. We assume that both solvents are good solvents for the polymer: the monomers of the chains have amphiphilic properties. When the minority solvent B is the better solvent, it is possible to find a preferential uptake of the solvent B. This solvent uptake can either occur in a continuous manner or in a first-order transition. From a wetting perspective, such a stepwise increase in B uptake may be identified as a prewetting step. In this case, however, the step is not necessarily caused by specific interactions with the solid substrate, but it results from an instability in the structure of the polymer brush at intermediate compositions of A and B in the brush. It is not always true that at coexistence the substrate is completely wet by the minority solvent, even when there is a prewetting step. We examine the post-transition solvent uptake up to and beyond the bulk binodal (in the case of partial wetting). The numerical SCF results complement a recent analysis of the same problem by a model of the Alexander−de Gennes type. Both in the numerical and in the analytical models, it is observed that the first-order phase transition is unusual: the polymer chains absorb the better solvent and then suddenly collapse to a very dense sublayer when there is only a small amount of the wetting component.

Introduction

Polymer brushes have received much attention from the scientific community in recent years. This can be attributed in part to the important applications for systems where control of surface properties is essential.[1,2] Typical key words are colloidal stabilization, antifouling coatings, and lubrication. Another reason for the recent interest in polymer brushes can be traced back to the fact that relatively simple analytical treatments of the system are very successful in describing the main properties.[3,4] Owing to this, brushes can serve as a testing ground for a wider area in polymer physics such as microgels. In practice, applications typically involve many components. For example, one can encounter a polymer brush system in an apolar solvent. Then, it may prove difficult to avoid having traces of water present in the system. Although the amount of water may well be below the saturation value, its effect on the brush properties may still be significant. Thus, the practical situation is characterized by a polymer brush in a mixture of two solvents. This is the topic of the present paper.

This paper continues the theoretical investigation of polymers which exhibit both hydrophilic and hydrophobic properties on the scale of a single monomer. Owing to this feature, they can be dissolved in incompatible liquids. Poly(ethylene oxide) is a familiar example of this type of polymers since it can be dissolved in water as well as in organic liquids. We thus consider polymer brushes immersed in a mixture of incompatible liquids. This system as an object of theoretical investigation was proposed by De Gennes.[5] Polymer chains are grafted to the plane surface at an area per molecule σ. All interactions are described by Flory−Huggins parameters. Since the solvent components are incompatible, their interaction parameter χ_{AB} should be greater than 2. Taking a strongly incompatible water (B)−oil (A) type system as an example, we set $\chi_{AB} = 3.5$. Interactions of the solvent components A and B with the polymer are described by parameters χ_{PA} and χ_{PB}. Both components are supposed to be good solvents for polymer, and $\chi_{PB} < \chi_{PA} < {}^1/_2$. This condition defines component B as a better solvent for the polymer as compared to component A.

The "exact" self-consistent field (SCF) method has been used for investigating these types of polymer systems.[6,7] The results show interesting effects on the brush structure and are nontrivial from a wetting point of view. However, the set of parameters chosen in ref 7 was such that the results partly correspond to systems that are supersaturated, whereas in ref 6 only relatively short chains are considered. A detailed study of the system has been recently performed in a rather general form[8] using the simpler Alexander−de Gennes boxlike model.[9,10] In this model all the chain ends are at the box boundaries, and the segment densities are assumed to be homogeneous. The brush height (box size) is adjusted until the stretching of the chains is in balance with the excluded-volume interactions. Evaluation of the chemical potentials in such a system allows one to identify the two phases that can coexist at the phase transition.

We are interested in SCF solutions for these systems to confront them with those obtained using a much simpler boxlike model. This allows us to receive a general view including both wetting and structural aspects of the problem.

[†] Russian Academy of Sciences.
[‡] Wageningen University.

10.1021/ma9910888 CCC: $19.00
Published on Web 01/22/2000

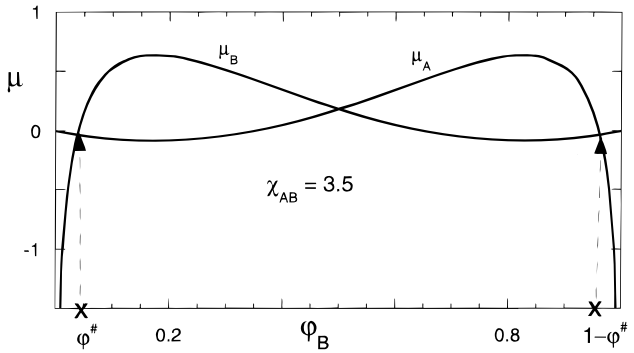

Figure 1. Chemical potentials of A and B components in a homogeneous A + B mixture, $\chi_{AB} = 3.5$. The crosses and arrows indicate the binodal points. The pure solvent is used for the reference of the chemical potential.

In the remainder of this paper, we first briefly discuss the main results of the investigation of the boxlike model of the system. Then some aspects of the wetting theory are reviewed. This is followed by a short outline of the numerical SCF theory. In the Results and Discussion section, we discuss a few typical cases already considered in the box model. As we will show the Alexander−de Gennes approach is doing a good job in predicting the position of the first-order phase transition as well as the magnitude of the step in solvent uptake. The features that take place at the bulk binodal value are however more accurately captured by the numerical method.

Review of Previous Results of the Box Model[8]

Let us describe briefly the results of the previous investigation[8] obtained for an Alexander−de Gennes boxlike model of a brush in an incompatible solvent mixture.

The mixture of the components A and B (in the bulk, outside the brush) can exist in a single phase only in the narrow concentration ranges $\varphi_B < \varphi_B^{\#}$ and $1 - \varphi_B^{\#} < \varphi_B$ where φ_B is the concentration of the component B in the mixture. Figure 1 shows the chemical potentials of the monomeric components A and B at $\chi_{AB} = 3.5$ as a function of the volume fraction of B in the system. As the bulk system is completely symmetrical, the chemical potentials of A and B must be equal. Equivalently, one can dissolve the same amount of A in the bulk B as the other way around. Equating the chemical potentials of A and B, we then can deduce the limiting concentration corresponding to the single phasic mixture in the bulk (binodal values) $\varphi_B^{\#} = 0.03787$ and $1 - \varphi_B^{\#} = 0.03787$; cf. Figure 1.

The main rearrangements in the brush structure occur when the bulk is in the single phase. The higher affinity of the minor solvent B to the polymer is a necessary condition of the process, $\chi_{PB} < \chi_{PA}$. If the brush is immersed in the pure solvent A, it is assumed to develop a uniform polymer concentration $\varphi_p^{(A)}$. The thickness of the brush is given by $H^{(A)} = N/\sigma\varphi_p^{(A)}$. Addition of component B to this system leads to a solvent exchange inside the brush, while the bulk remains a single phase with very low concentration of B. When the chemical potential of the solvent reaches the binodal value, the solvent inside the brush is changed and the segment density equals $\varphi_p^{(B)}$ (in the absence of solvent A); the brush thickness is given by the relation $H^{(B)} = N/\sigma\varphi_p^{(B)}$. Further addition of the component B does not affect the brush structure, while the phase segregation of the solvent outside the brush is observed. What happens is that there will be a growth of the wetting film composed of the B-rich solvent on top of the unperturbed brush.

The process of the solvent exchange inside the brush can develop in different ways, depending on the area available per grafted molecule σ and the values of χ_{PA} and χ_{PB}. The solvent composition changes either smoothly or as a phase transition and is accompanied by major rearrangements in the brush structure. Three different scenarios are found.

(i) If solvent A is relatively poor and the brush is collapsed so that the segment density $\varphi_p^{(A)}$ is high, addition of solvent B leads to a continuous solvent exchange. The segment density decreases monotonically (brush height increases) with amount of added B, until the system reaches the (lower) limiting value $\varphi_p^{(B)}$. This continuous uptake of solvent B is typical for dense systems, i.e when $\varphi_p^{(A)}$ is rather high. Thus, the better the solvent A is for the polymer, the more densely grafted the system must be in order to observe this process.

At good solvent conditions and at relatively low values of the initial segment density $\varphi_p^{(A)}$, the addition of solvent B causes a nonmonotonic change in the brush structure; e.g., the brush height H first decreases and then increases again. At a certain concentration of component B in the bulk, a sudden solvent rearrangement inside the brush takes place and the brush collapses into the newly formed film which is rich in B. This process occurs either (ii) in a continuous manner or, at sufficiently low values of the initial segment density, as a (iii) phase transition. In the latter case, especially when the newly formed B phase is just microscopically thin, microphase segregation of the polymer brush segments is observed: there are two sublayers in the brush. Near the grafting surface, a collapsed sublayer is filled by the solvent B, while at the outer boundary the brush is swollen in the solvent A. A sharp A−B interface separates the two microphases. The segment density in the collapsed phase is homogeneous and this density is a function of σ, χ_{PA}, and χ_{PB}. If the amount of component B happens to be sufficient to fill the whole brush with the appropriate density, the brush is in a single collapsed phase.

With further increase in the concentration of component B, the brush swells in this solvent (provided that the solvent B is sufficiently better than A). The segment density decreases until it reaches the value $\varphi_p^{(B)}$ at $\varphi_B = \varphi_B^{\#}$.

All these effects were obtained in a framework of a simple boxlike model of the bush. This model has the great advantage that analytical relations are obtained so that the system can be investigated rather generally. However, it highly overestimates the system homogeneity and neglects all boundary effects. Since these effects are of a significant interest, numerical calculations are useful to complement the picture.

Classical Wetting Theory

To appreciate the results for the system under considerations, it is expedient to review also briefly some basic points of the classical wetting theory (see, e.g., ref 11 for a more thorough review). Upon the approach of a solubility gap in the bulk of a two-component solvent

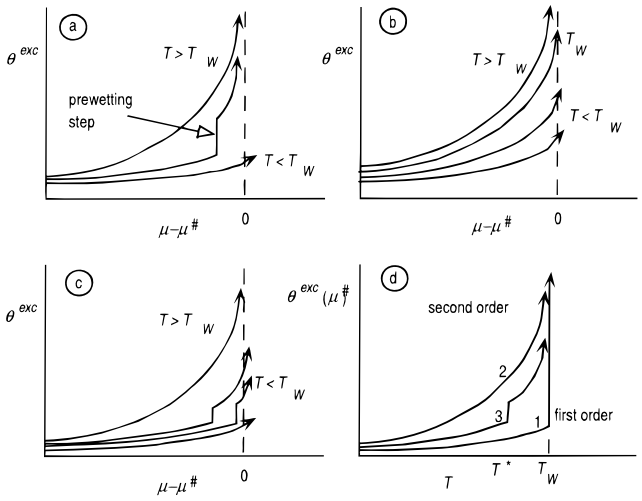

Figure 2. Typical families of adsorption isotherms, giving the excess adsorbed amount θ^{exc} (in equivalent monolayers) as a function of the normalized chemical potential $\mu - \mu^{\#}$. Here, $\mu^{\#}$ is the chemical potential at bulk coexistence. Curves are drawn schematically for three wetting scenarios: (a) first-order wetting, (b) second-order wetting, and (c) second-order wetting in combination with a prewetting step. In viewgraph d the adsorbed amount at bulk coexistence (binodal) is plotted as a function of the control parameter (in this case the temperature). Curve 1 corresponds to the first-order wetting case (a), curve 2 to the second-order wetting case (b), and curve 3 is a curve as can be found for wetting of a polymer brush; it corresponds to situation c. T_W is the wetting temperature and T^* is the temperature where two film thicknesses can coexist with a macroscopic droplet.

mixture, the system must move from a single phase to two phases. The new phase can occur somewhere in the bulk of the solution (homogeneous nucleation), but also near existing interfaces (heterogeneous nucleation). We will be interested in the latter scenario. Basically we can distinguish two cases. The new phase can sit as a droplet at the interface, or the new phase can cover the interface completely by forming a homogeneous film. The latter instance is referred to as *complete* wetting, the first one to *partial* wetting. Transitions from partial to complete wetting are of special interest. Wetting transitions can occur in two ways: they are either first or second order. The difference between the two can most easily be illustrated by examining adsorption isotherms of the wetting component onto the substrate as a function of the control parameter. For the case of simplicity we choose here the temperature T to be the control parameter, but below we will use some specific Flory−Huggins interaction parameter for this purpose. Schematic representations of the relevant scenarios are collected in Figure 2. In parts a−c of Figure 2, we give adsorption isotherms, i.e., the excess adsorbed amount of the wetting component as a function of the chemical potential μ of this component. This last quantity is normalized with respect to the binodal value $\mu^{\#}$. Only those parts that are below the bulk binodal are sketched. In the limit of infinite adsorbed amount all isotherms merge to $\mu - \mu^{\#} = 0$. In Figure 2d the adsorbed amount at coexistence ($\mu = \mu^{\#}$) is plotted as a function of the control parameter in the system.

The family of adsorption isotherms as shown in Figure 2a, and the curve 1 in Figure 2d are typical for a first-order wetting transition. The special features in Figure 2a are that for $T < T_W$ the system is partially wet and the isotherm crosses the bulk binodal at a finite value, whereas for $T > T_W$ the adsorption isotherms diverge upon the approach of the bulk binodal. For temperatures T just above the wetting transition, there is a jump in adsorbed amount. At this point, a microscopically thin wetting film transforms into a mesoscopically thick one in a first-order transition. Note that this occurs at $\mu < \mu^{\#}$. It is of interest that after the jump in the adsorbed amount, the isotherm diverges upon the approach of the bulk binodal. In a family of adsorption isotherms, one can study the features of the jumps, usually referred to as prewetting steps, in the isotherms. The closer the jump occurs to $\mu^{\#}$, the larger in size will be the jump. When the jump occurs at $\mu = \mu^{\#}$, the step is infinitely large. Correspondingly, the adsorbed amount at coexistence, curve 1 in Figure 2d, remains finite below the wetting transition and it is infinite above the transition. The infinite jump in adsorbed amount at the wetting temperature is typical for the first-order character of the event.

Figure 2b and curve 2 in Figure 2d are typical for a system that exhibit a second-order wetting transition. In this case there are no prewetting steps in the isotherm. Below the wetting transition, $T < T_W$, all isotherms cross the bulk binodal at some finite value of the adsorbed amount, and when $T > T_W$, the isotherms do not cross $\mu = \mu^{\#}$. As shown in Figure 2d, the film thickness at coexistence grows smoothly upon the approach of the wetting transition. This smooth divergence is characteristic for a second-order wetting transition.

In Figure 2c and curve 3 in Figure 2d a nonclassical case is shown (for example, this case is not discussed in ref 11). This situation is typical for the wetting of a polymer brush, as we will encounter below. The isotherms have features of the case discussed in Figure 2a, because there is a prewetting step, but also aspects of Figure 2b, because the wetting transition is second order. Characteristic for the wetting scenario of Figure 2c is that a prewetting step exists in the temperature range $T < T_W$. This can be seen from the fact that an isotherm which has a step crosses the bulk binodal at some *finite* value of the excess adsorbed amount. It is possible to find a special temperature T^*, for which the step in the adsorption isotherm occurs at the bulk coexistence point. This is a special point, as in this case three states can coexist, namely, a microscopic and a mesoscopic film and a macroscopic droplet.

The Scheutjens−Fleer Self-Consistent-Field Theory

There are many different levels of mean-field theories to describe polymer brushes. The Alexander−de Gennes box model used in the previous paper[8] is probably the most basic one. More advanced models make use of the fact that the potential profile $u(z)$ felt by the grafted polymer chains is often to a good approximation parabolic.[2−4] The exact mean-field model for polymer brushes, however, is based on the Edwards diffusion equation:[12]

$$\frac{\partial G}{\partial s} = \frac{1}{6}\frac{\partial^2 G}{\partial z^2} - uG \qquad (1)$$

Here $G(z,s|z',s')$ is a Green's function which represents the statistical weight of all possible and allowed "walks" of $s - s'$ segments long which have segment s at coordinate z and s' at coordinate z'. The appropriate starting condition is $G(z,0|z,0) = \delta_z$ (segment $s = 0$ is at $z = 0$). We use the discrete version of this equation,

which is known as the Scheutjens-Fleer self-consistent-field variant.[13] The discretization is done both with respect to the contour of the polymer chain and with respect to the spatial coordinate: the chain is assumed to be composed of segments with length b, numbered $s = 1, ..., N$, and the volume is subdivided in cells, each also of size b. These cells are arranged in a regular lattice with layers numbered $z = 1, ..., M$, where layer 1 is the first layer next to an impenetrable solid substrate. Layer $z = M$ is situated far from the substrate where all inhomogeneities have died out and bulk conditions prevail. Note that we use the letter z both for the continuous spatial coordinate and for the discrete analogue (layer number). The Edwards diffusion equation transforms now into a set of relatively simple recurrence relations:

$$G(z,s|1,1) = G(z,s)\langle G(z,s-1|1,1)\rangle \quad (2a)$$

$$G(z,s|N) = G(z,s)\langle G(z,s+1|N)\rangle \quad (2b)$$

where we introduced angular brackets which give a three-layer average over the argument

$$\langle G(z)\rangle = \lambda G(z-1) + (1-2\lambda)G(z) + \lambda G(z+1) \approx G(z) + \lambda b^2 \frac{\partial^2 G(z)}{\partial z^2} \quad (3)$$

which depends on a lattice parameter $0 < \lambda < 0.5$. In the Green functions, we specify the starting conditions of the walk by the arguments following the vertical bar. It is understood that $G(z,s|N) = \sum_{z'} G(z,s|z',N)$. The starting conditions for eq 2 are $G(z,1|z,1) = \delta_{z-1}G(z,1)$ and $G(z,N|N) = G(z,N)$. Here and in eq 2 we use $G(z,s) = \exp(-u(z,s))$, which is the Boltzmann weight featuring the dimensionless segment potential in its argument. They represent the statistical weight of finding segment s in the system if it were unconnected to the chain. The segment densities $\varphi(z,s)$ of the grafted chains are found by a composition formula:

$$\varphi(z,s) = \frac{1}{\sigma G(1,1|N)} \frac{G(z,s|1,1)G(z,s|N)}{G(z,s)} \quad (4)$$

Here the division by $G(z,s)$ needs to be included to correct for the fact that the segment potential of segment s is included both in $G(z,s|1,1)$ and in $G(z,s|N)$.

To this point, we have assumed that there is one type of segment. However, as mentioned above, the system contains not only polymer segments but also solvent molecules. In this case there are two types of solvent, A and B, and therefore there are three types of segment: x = P, A, B. The three segments differ only with respect to the nearest neighbor interactions, not with respect to their size. There are three Flory−Huggins parameters χ_{PA}, χ_{PB}, and χ_{AB}. Moreover there is a solid substrate x = S. This segment type is present with a density of unity in layers $z \le 0$ only. The Flory−Huggins interaction parameters linked to the interactions of the substrate with the solvent are also three: χ_{SA}, χ_{SB}, and χ_{SP}. Having specified the interaction we can now give the segment potentials as

$$u_x(z) = u'(z) + \sum_{y=P,A,B,S} \chi_{xy}(\langle\varphi_y(z)\rangle - \varphi_y^b) \quad (5)$$

where it is understood that $\chi_{xx} = 0$, and $u_P(z) = u(z) = u(z,s)$ as used above (each segment s in the chain is of segment type P) and $\varphi_p(z) = \sum_s \varphi(z,s)$. In eq 5 $u'(z)$ is a Lagrange field coupled to the constraint that in each layer z the volume fractions add up to unity (incompressibility constraint): $\sum_x \varphi_x(z) = 1$. Finally, in eq 5 we have introduced the density of segment type y in the bulk, φ_y^b, for normalization purposes only. The densities of the two solvents are computed by $\varphi_B(z) = C_B \exp(-u_B(z)) = C_B G_B(z)$. The normalization C_B is fixed by the amount of B in the system $\theta_B = \sum_z \varphi_B(z)$. This means that $C_B = \theta_B/\sum_z G_B(z)$. It is also easily seen that $C_B = \varphi_B^b$ as in the bulk all weighting factors are equal to unity. The normalization of component A simply follows from the condition that the densities in the bulk add up to unity as well: $C_A = \varphi_A^b = 1 - \varphi_B^b$. Below we will use the case that the two solvents A and B strongly segregate: $\chi_{AB} = 3.5$. This results in an interfacial width comparable to the lattice spacing b. In systems which such sharp interfaces the best choice for the lattice parameter is $\lambda = 1/3$ (representing a fcc lattice). This choice results in less so-called lattice artifacts as compared to other lattice types.

At this point, the set of equations is closed, and a numerical procedure is used to find the fixed point of the equations. For such a point one can compute segment potentials from given segment volume fractions. From these potentials it is possible to recover the original segment densities within a precision of typically seven significant digits.[14] Recall as well that the incompressibility constraint is obeyed within the same type of precision. For a given SCF solution, it is possible to evaluate structural information (i.e., density profiles) as well as thermodynamical information (by way of the partition function).

Results of Numerical SCF Calculations

In the following, we will not attempt to cover a similar range of parameters as was done within the box model. Instead we will try to evaluate how well the physics of the box model coincides with the more exact lattice calculations. Typically we will consider, inspired by the results of the box model, the following set of the parameters. As before, the solvent components A and B are highly incompatible: $\chi_{AB} = 3.5$. We recall that $\varphi_B^\# = 0.03787$ (corresponding to $\mu_B^\# = -0.4469$; here and below we will use the pure solvent as the reference for the chemical potential) is the critical value of the concentration in this mixture; see Figure 1. Component A is a good solvent for the polymer and we consider two values of the interaction parameter, viz. $\chi_{PA} = 0.3$ and $\chi_{PA} = 0$. Component B is a better solvent than A and the values $\chi_{PB} = 0$ and $\chi_{PB} = -2$ are used. Two different values of the area per molecule of the nonreversibly grafted molecules ($\sigma = 50$ and $\sigma = 250$) are chosen. All calculations are carried out for a chain length $N = 500$, and the number of lattice layers was fixed to $M = 400$.

We note that above we have used the temperature as the control parameter to influence the wetting characteristics of a particular system. In the present type of systems, the change in temperature is reflected in the change in Flory−Huggins interaction parameters. In principle, a temperature change will influence all interaction parameters simultaneously. Below we will assume that it is possible to change the interaction parameters independently.

Unless specified otherwise, we will use an inert solid substrate, which shows no preferred interactions with any of the molecular species, A, B, and P. In the absence

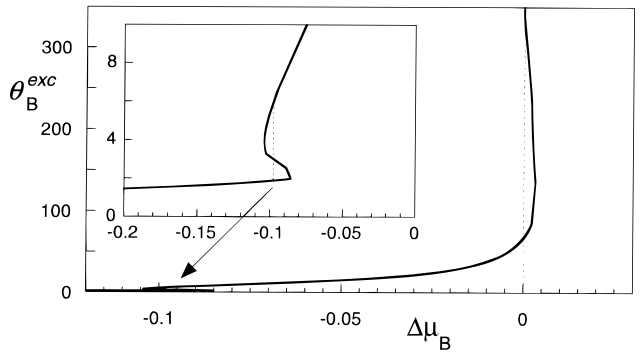

Figure 3. Adsorption isotherm of solvent component B at surface covered by polymer chains with grafting density $\sigma = 50$. The Flory−Huggins interaction parameters are $\chi_{AB} = 3.5$, $\chi_{PA} = 0.3$, and $\chi_{PB} = 0$. The chemical potential is normalized with respect to the value at bulk coexistence. The dashed line at $\Delta\mu_B = 0$ is an aid for the eye inserted to show that the adsorption isotherm crosses the binodal. In the inset the adsorption isotherm in the prewetting step region is enlarged.

of a polymer brush, i.e., the solid substrate in the presence of A and B only, the system at coexistence is obviously partially wet. The drop of the wetting component on the substrate will have a contact angle of 90°. This is easily seen by realizing that in this symmetric case the surface attracts the bulk rich in A as strong as the bulk rich in B.

1. Wetting. In Figure 3, a typical adsorption isotherm is given. In this example $\chi_{PA} = 0.3$, $\chi_{PB} = 0$, and $\sigma = 50$. In this isotherm the excess adsorbed amount, defined by $\theta_B^{exc} = \sum_z(\varphi_B(z) - \varphi_B^b)$, is plotted as a function of $\Delta\mu_B = \mu_B - \mu_B^{\#}$. Since the isotherm crosses the binodal value $\Delta\mu_B = 0$ at a fixed value of θ_B^{exc}, it corresponds to partial wetting. This is seen by the fact that the system is, for a significant range in θ_B^{exc} ($67 < \theta_B^{exc} < 340$), in the supersaturated domain, $\Delta\mu_B = 0$. When $\theta_B^{exc} > 340$, the system is in the stable state again and $\Delta\mu_B = 0$. At coexistence there is a given amount of solvent B trapped in the brush ($\theta_B^{exc} \approx 67$). At presaturation conditions (low θ_B^{exc}) a van der Waals loop shows up in the adsorption isotherm. The Maxwell construction may be used to determine the corresponding step in the isotherm. In light of the classical wetting theory as outlined above (parts a and b of Figure 2), this is unexpected: for partial wetting conditions, corresponding to the classical picture there should be no prewetting step in the adsorption isotherm!

A more thorough analysis of this system reveals that the wetting transition in Figure 3 is not first but second order. This follows from the fact that the adsorbed amount of B at coexistence diverges smoothly upon the approach of the wetting transition. We address this issue in a separate publication.[6] This again is remarkable because for a second-order transition no prewetting step in the isotherm is present in the classical theory (cf. Figure 2b and Figure 2d, curve 2). Clearly the brush system obeys a wetting scenario as sketched in Figure 2c and Figure 2d, curve 3. In fact, the prewetting step observed for brushes is not directly linked to the wetting transition. It is generated by an instability of the polymer brush and gives no direct indication about the nature of the wetting transition. It is noteworthy that in the box model no peculiarities were observed in the vicinity of $\Delta\mu_B = 0$. However, the order of the wetting transition is not the issue of the present paper, and we refer the reader to the literature for more details.[6] We

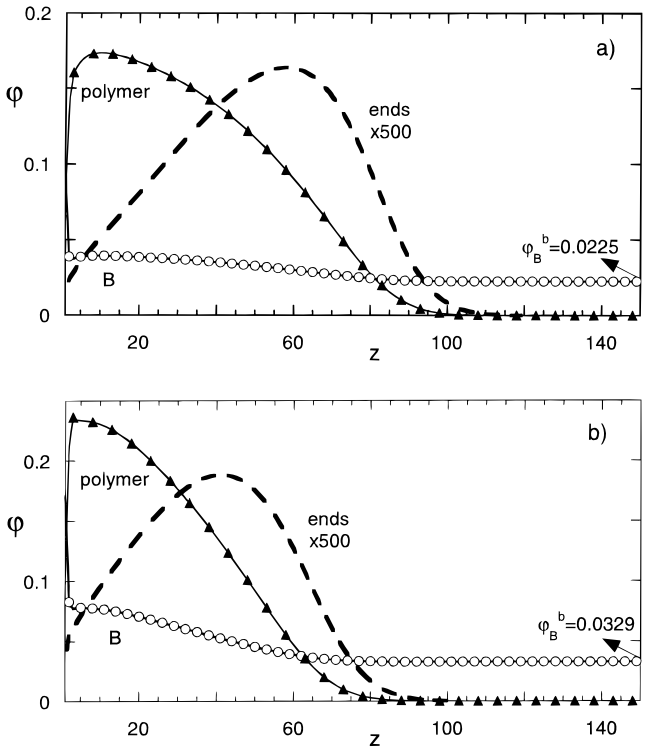

Figure 4. Density profiles of the polymer segments, the wetting solvent B and those of the grafted chain ends for low concentrations B: (a) $\theta_B^{exc} = 0.98$; (b) $\theta_B^{exc} = 1.82$. All other parameters are the same as in Figure 3.

focus below on the structure rearrangements within the brush caused by the addition of the minor component B.

2. Structure of the Brush. Let us now address the structural properties of the brush in the mixed solvent corresponding to the case shown in Figure 3. This case (with the same parameters) has been examined in detail in the box model.[8] At $N/\sigma = 10$, the system is well in the brush regime; in a single solvent, the end-attached chains are strongly stretched: $H \propto N$. From inspection of the adsorption isotherm in Figure 3, we know that this is a case with an evident phase transition. This phase transition shows up as a van der Waals loop in the isotherm. As the van der Waals loop is rather small, we mention that the system is close to the critical point for this prewetting transition. We may distinguish five regions in the isotherm: (i) a pre-transition concentration range, (ii) the brush collapse (transition point), (iii) the post-transition swelling of the brush up to the bulk coexistence value, (iv) the supersaturated region (located at $\Delta\mu_B > 0$), and finally (v) the fully submerged brush.

In the pre-transition concentration range, the solvent B is present in very low concentration and the structure of the brush is almost as in pure A. This is illustrated in Figure 4, which presents the polymer density profile and the density profile of the free ends of the polymer chains as well as the concentration profile of the wetting solvent B. In Figure 4a, the bulk concentration of component B is $\varphi_B^b = 0.0225$ ($\Delta\mu_B = -0.448$), whereas in Figure 4b it is slightly higher: $\varphi_B^b = 0.0329$ ($\Delta\mu_B = -0.14$). The concentration of B is such that there is only an accumulation of B at the substrate: the excess adsorbed amounts of B on the surface are $\theta_B^{exc} = 0.985$, and $\theta_B^{exc} = 1.82$, respectively (not shown on the scale of parts a and be of Figure 4). That is, just near the surface

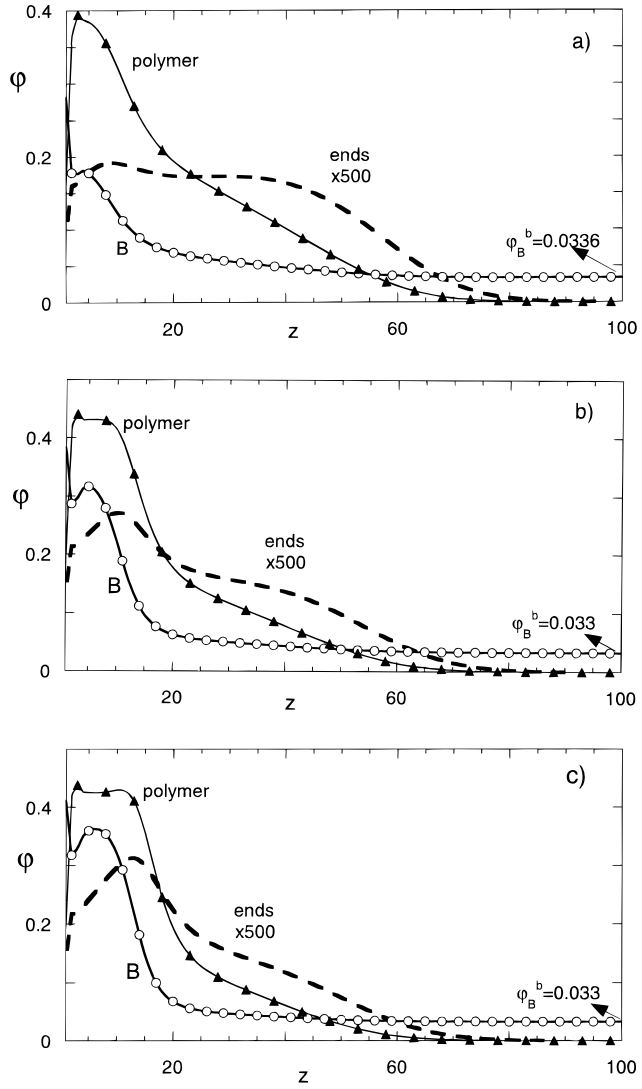

Figure 5. Density profiles of polymer segments, the wetting solvent B and of the grafted chain ends in the transition region of Figure 3, for (a) $\theta_B^{exc} = 2.54$, (b) $\theta_B^{exc} = 3.80$, and (c) $\theta_B^{exc} = 4.77$. All other parameters are the same as in Figure 3.

there is a steep increase in density of B. This is due to the fact that the solvent has an effective adsorption energy due to the presence of the depletion layer of the polymer near the substrate. The density profile of B at higher z is only slightly higher than the bulk value. The most interesting effect, however, is found for the polymer profile. Comparison between parts a and b of Figure 4 clearly shows that the polymer brush compresses somewhat the wetting component, and B is of better thermodynamic quality for the polymer with an increasing amount of the wetting component. This is noteworthy because with increasing average concentration of B, the average solvent quality improves. No fundamental rearrangement of the brush structure is observed however in this range of the mixture composition: the profiles remain parabola-like. The free end distribution remains smooth and shows no special singularities.

The structure of the polymer brush changes dramatically at the transition point (prewetting step at the adsorption isotherm). In Figure 5 we show three typical density profiles of brush systems within the van der Waals loop region of the adsorption isotherm. Parts a−c of Figure 5 clearly demonstrate the brush collapse. The three systems correspond to subsequent increases in the amounts of molecules B added to the system. In parts a−c of Figure 5, these amounts are 16, 17, and 18 molecules per lattice site ($M = 400$). The corresponding excess amounts of solvent B in the system are θ_B^{exc} 2.54, 3.8, and 4.77 in parts a−c of Figure 5, respectively.

It is significant that the end-point distribution of the grafted polymers has now two maxima, one at approximately the same position as in Figure 4, with the new one near the substrate. This kind of singularity in the free end distribution is typical of the microphase segregation and does not depend on the causes of segregation.[15,16]

Roughly speaking, there are two populations of chains. One population is collapsed in a region $z < 10$, and the other is still parabolic like in Figure 4. Note again that the collapsed chains are in the better solvent B, and the extended chains are in the poorer solvent A. Clearly the brush is microphase segregated. The polymer segment density in the solvent B (the collapsed phase) is rather high (of order 0.4), is almost constant over the collapsed region, and is independent of the amount of solvent B in the system (compare parts a−c of Figure 5).

The profile of the wetting solvent B follows the polymer profile. It is only slightly increased with respect to the bulk in the outer part of the brush region, whereas it has a much higher density in the part of the brush where the polymer is collapsed. Very close to the substrate boundary, a further increase of the solvent B density is found, which again can be attributed to filling up the depletion layer of the brush. It is of interest that the solvent density in the collapsed region remains lower than the polymer density.

In the previous publication[8] the collapse as illustrated in Figure 5 was called "anomalous". Indeed, for a polymer brush existing in equilibrium with a single-component solvent, the polymer concentration in a brush is a decreasing function of solvent strength, i.e., $\varphi_p^{(B)} < \varphi_p^{(A)}$ at $\chi_{PB} < \chi_{PA}$. However, in the present case of an incompatible two-component solvent mixture, the opposite situation is observed: $\varphi_p^{(B')} > \varphi_p^{(A)}$ at $\chi_{PB} < \chi_{PA}$ (here the prime on (B′) reminds us of the fact that the polymer sits in the B phase which is just microscopic in size since $\mu_B < \mu_B^{\#}$).

If component B is added in sufficient concentration to fill up the whole brush, the microphase segregation does not exist any longer. In Figure 6 we examine this domain of swelling of the polymer brush (post-transition swelling), including profiles that correspond to supersaturation (see Figure 3) and a fully submerged brush. The stable curves are drawn as solid curves; the unstable (supersaturated) ones are dashed. In Figure 6a, we collected the overall polymer density, in Figure 6b, we present the end point distributions, and in Figure 6c, the profiles of the wetting component B are given. The various curves in Figure 6 correspond to increasing amounts of wetting component in the system, as indicated in the legend. For the lowest value of the wetting component, we observe still some indication of the microphase segregation as found in the transition region.

Upon increasing amounts of the wetting solvent we find basically four effects characterizing the change in the overall density profiles. (a) The polymer density near the surface relaxes gradually toward lower values. (b) The shape of the polymer density profile gradually changes from a homogeneously collapsed one to the parabolic profile in a good solvent. (c) A significant

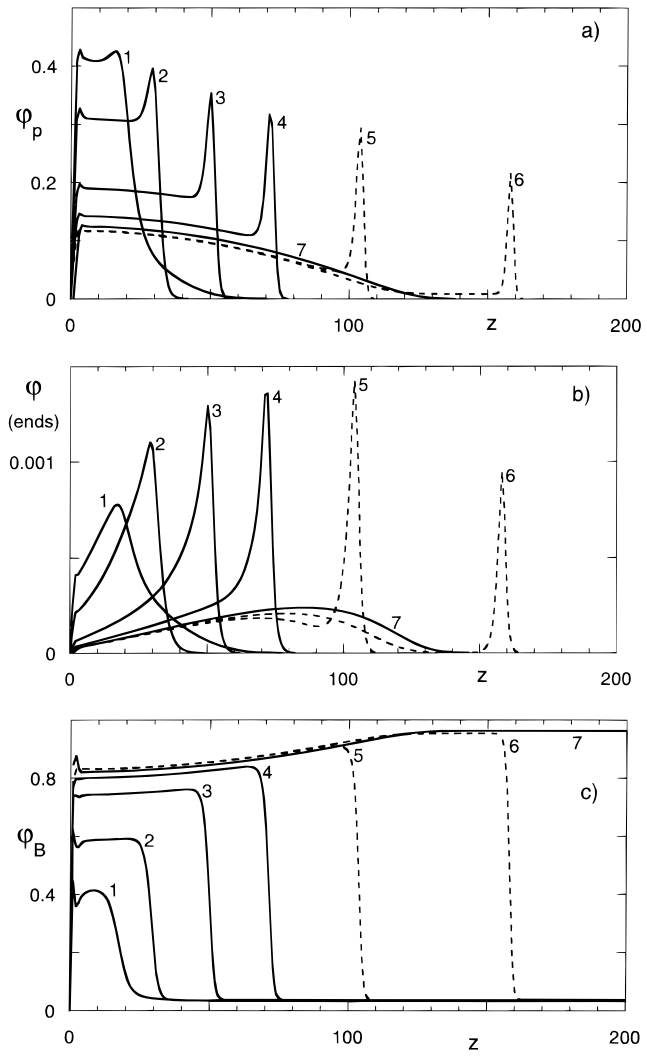

Figure 6. Density profiles of (a) polymer segments (b) end segments of the grafted chains and (c) wetting solvent B at high concentrations of the wetting solvent B. The numbers 1−6 refer to θ_B^{exc} = 6.64, 15.77, 35.11, 54.92, 84.82, and 134.80, respectively. Number 7 is typical for a sufficiently large value of θ_B^{exc} such that the brush is fully submerged. All other parameters are as in Figure 3. We have made the lines dashed for the density profiles for those systems that are in the supersaturated domain.

amount of polymer adsorbs at the A−B interface. This shows up as a sharp peak in the outer part of the brush. The adsorption is due to the fact that the polymer segments can screen the unfavorable A−B contacts (reduction of interfacial tension of the A−B interface). (d) At relatively large amount of wetting solvent in the supersaturated domain there is a new feature: a stem appears between the adsorption maximum present at the A−B interface and the parabolic region. The stem is a result of extra stretching of some of the polymer chains. With increasing amount of wetting solvent, the population of chains which take part in this extra stretching reduces until eventually the brush chains can no longer reach the A−B interface. The accumulation of chain segments at the A−B interface was shown and discussed previously.[6,7]

In the box model a similar post-transition swelling was observed, but the interfacial adsorption effects, including the formation of a stem, could not be investigated. Further, it is rather difficult to evaluate in a box model the crossing of the binodal especially when the amount of good solvent B is sufficient to fully develop the polymer brush in this solvent. Therefore, the box model is not appropriate to discriminate between wetting and partial wetting cases and to study wetting transitions.

The end-point distributions shown in Figure 6b are of interest as well. For the lowest amount of added wetting solvent B in this figure, there is a strong maximum near $z = 20$, but also a shoulder at higher z, which is a remainder of the biphasic nature of the transition discussed in Figure 5. With increasing amount of wetting component B, the shoulder is lost and the end-point distribution becomes sharply peaked at the edge of the brush (i.e., near the A−B interface). Just before we reach the development of the stem in the overall profile, we notice that the end-point distribution develops a shoulder at intermediate z values. This event signals the fact that the system is going to cross the bulk binodal. When the stem is fully developed (i.e., when the system is in the supersaturated state), the end-point distribution again shows two distinct maxima. The brush is thus again biphasic. One population of the chains is disconnected from the A−B interface and gives rise to the parabolic density profile. The other population is even more stretched and reaches out for the A−B interface. This relative importance of the end-point maxima gradually shifts back toward the normal end-point distribution corresponding with a parabolic density profile: the singularity of the end-point distribution at the A−B interface is then lost. Now all chains have relaxed back into conformations typical for an unperturbed brush in the good solvent B.

The profile of the wetting solvent B is given in Figure 6c. In line with the changes in the overall profile of the polymer segments, we observe first an increase in density of the solvent B. Also it relaxes from a rather homogeneous density as long as the brush is still compressed to a profile complementary to the polymer brush profile. The drop of the B density indicates the position of the A−B interface. For higher distances from the wall, the space is mainly filled by solvent A. The width of the A−B interface initially sharpens slightly. This is due to the gradual loss of the biphasic region of the polymer moiety. This width then becomes of order of the molecular size b (the width of the A−B interface can be controlled by adjusting the χ_{AB} parameter). The fact that the chemical potential of the solvent B crosses the bulk binodal cannot easily be deduced from these graphs as the degree of super-saturation is very small indeed. As soon as the A−B interface detaches from the brush, the chemical potential of the solvent B has relaxed to the binodal value.

One may wonder what the equilibrium state is of a system which is supersaturated. Obviously, the system is in this case metastable and cannot be realized physically. It is clear that these solutions of the SCF calculations correspond to local minima in the free energy, which only could be generated because the system was forced to be laterally homogeneous. If this constraint is released, the wetting solvent will be in fact distributed inhomogeneously along the interface:[17] most of the surface will be in the state where the brush is swollen by the wetting solvent to a degree consistent with the adsorbed amount of the wetting component at coexistence. The remainder of the solvent will be collected into a macroscopic large drop under which the brush does not see the liquid−liquid interface any

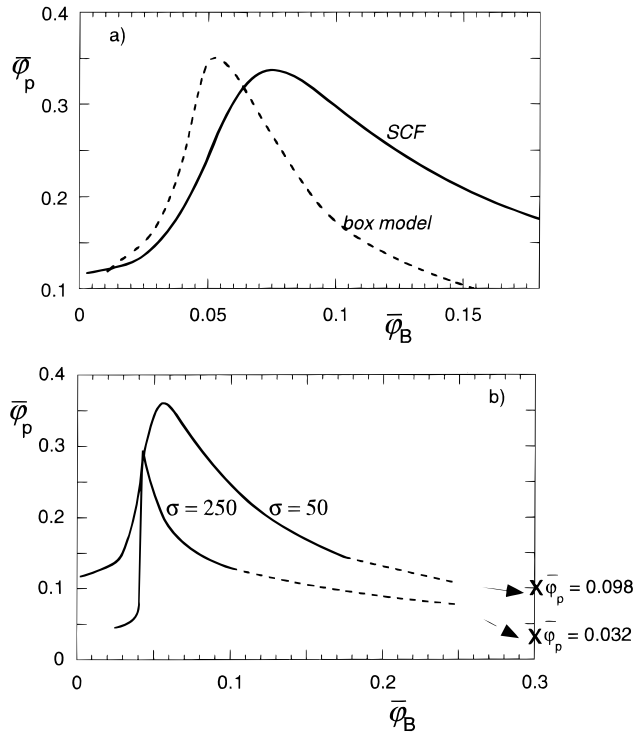

Figure 7. (a) Average polymer segment density in the brush $\bar{\varphi}_p$ vs average concentration of B component $\bar{\varphi}_B$ in the system for the same parameters as in Figure 3. Results obtained for the box model[8] are given by dashed lines. (b) Dependence of average segment density $\bar{\varphi}_p$ on average concentration of B component $\bar{\varphi}_B$ for a densely grafted system ($\sigma = 50$) and sparsely grafted one ($\sigma = 250$). The dashed parts of the curves correspond again to supersaturated systems. The extrapolated values for the polymer density in a B solvent are indicated.

longer. For this configuration the chemical potentials of the solvents are also given by the binodal values.

It is of interest to compare the results of the numerical calculations with those obtained for the box model.[8] To this end we define an average root-mean-square polymer density in the brush as

$$\bar{\varphi}_p = \frac{\sum_z \varphi_p(z)\varphi_p(z)}{\sum_z \varphi_p(z)} \qquad (6)$$

and the average concentration of solvent B in the system as $\varphi_B = \theta_B/M$, where the total number of layers M in the system was fixed to 400. In Figure 7a the average polymer density is plotted as a function of the average concentration of the component B in the whole system $\bar{\varphi}_B$ for both the box model and for the numerical SCF model. It is evident that both methods give rather similar results. The maximum in the curves corresponds to the collapse of the brush. This maximum is not very pronounced in this case. Thus, for the chosen set of parameters the transition may be characterized as being weak. The correspondence indicates that the box model is rather accurate for predicting prewetting phenomena at relatively low $\bar{\varphi}_B$. Figure 7b will be discussed below.

3. Wetting Aspects and Brush Structure for Two Other Systems. It was shown in the box model that the average polymer density in the system governs the collapse phase transition and the microphase segregation. To test this effect, we now consider a more diluted

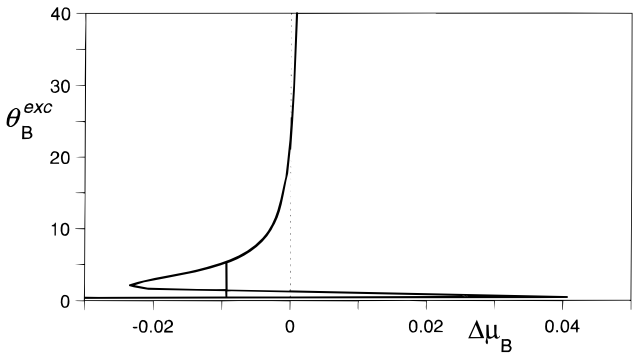

Figure 8. Part of the adsorption isotherm of solvent component B at surface covered by polymer chains with grafting density $\sigma = 250$. Other parameters are the same as in Figure 3. The dashed line indicates the bulk binodal, and the solid line in the isotherm corresponds to the prewetting step.

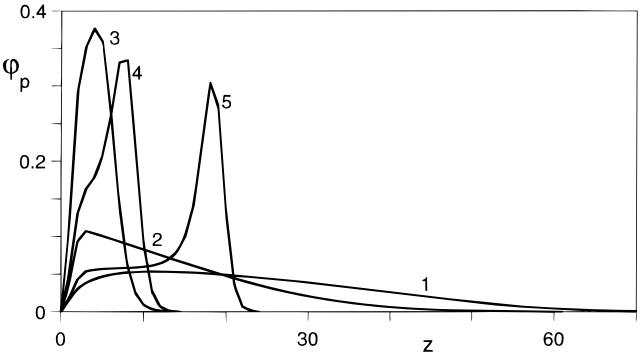

Figure 9. Overall segment density profile of the grafted polymers in the presence of a wetting solvent. The numbers 1−5 refer to θ_B^{exc} = 0.23, 8.47, 10.46, 12.44, and 24.43, respectively. All other parameters are as in Figure 8.

brush than in the previous figures: $\sigma = 250$. All other parameters are the same as in the previous viewgraphs. Figure 8 show the part of the adsorption isotherm near the prewetting step. It is seen that the brush collapses at approximately the same chemical potential of the wetting solvent as above. The van der Waals loop is now more pronounced than in the previous case (Figure 3). This means that the system is further away from the prewetting critical point. In terms of adsorbed amounts, the width of the biphasic region is approximately of the same size. Again the isotherm crosses the bulk binodal value. This means that also in this case the component B does not wet the interface completely. The amount of trapped solvent B at the bulk saturation is approximately $\theta_B^{exc} = 22$. The average polymer segment concentration at this point (shown in detail in Figure 9, curve 4) is close to the value found in Figure 6a. The average density of polymer segments in the brush is given by $\bar{\varphi} \propto \sigma N/H \propto \sigma^{2/3}$. This suggests that the amount of solvent B trapped in the brush obeys $\theta_B^{trapped} \propto \sigma^{2/3}$. The trapped amounts as cited above are consistent with this. When the amount of trapped solvent exceeds the capacity of the brush, we expect a wetting phase transition. Obviously we should have values $\sigma < 50$ to have complete wetting in this case. With decreasing σ the trapped amount increases smoothly (not shown) indicating that the wetting transition, as generated by decreasing σ, is robust second order. This is consistent with the findings of ref 6 and the sketched curve in Figure 2d, curve 3.

The overall structural properties of the brush systems of Figure 8 are presented in Figure 9, where we

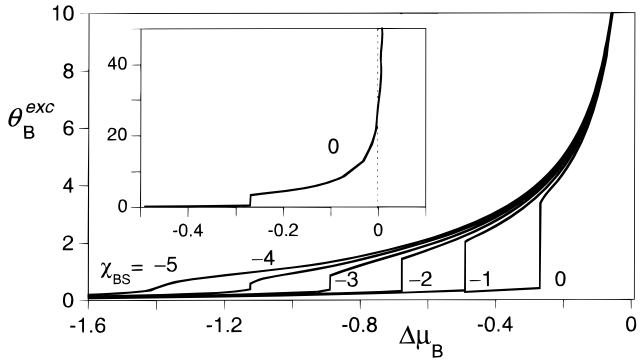

Figure 10. Adsorption isotherms near the prewetting transition region for various values for the adsorption energy of the wetting component B with the substrate S as indicated. The other parameters are $\chi_{AB} = 3.5$, $\chi_{PA} = 0$, $\chi_{PB} = -2$, and $\sigma = 250$. In the inset, we show a larger part of adsorption isotherm for $\chi_{BS} = 0$. The dashed line indicates the bulk binodal.

concentrate on the parameter space that corresponds to cases where the bulk is still in the one-phase region (only the stable region). The differences between the profiles shown above (polymer profiles in Figures 4 and 5 and Figure 6a, curves 1−4) and the ones in Figure 9 can easily be rationalized by the difference in grafting density. Typically in Figure 9 the density of polymer in the collapsed phase is a bit lower (cf. Figure 5b polymer profile). Also the adsorption peak at the liquid−liquid interface is less pronounced in Figure 9 compared to that in Figure 6a. The end point distributions (not shown) become again double peaked for the system near the collapse transition region, and it remains single peaked for curves 4 and 5 in Figure 9. In line with the above findings, again a double-peaked end-point distribution is found when the metastable wetting film is present (supersaturation).

In Figure 7b a comparison is made between low and high grafting density as to how the average polymer concentration changes as a function of the average amount of wetting solvent B in the system ($M = 400$). The average polymer density at the transition point is, in agreement with the results of the box model, not a strong function of the grafting density. From this graph it is further concluded that the collapse transition is more sharp in the case of sparse grafting (σ large). This correlates well with the extension of the van der Waals loops. Above, it was shown that the $\sigma = 250$ is further away from the prewetting critical point than the $\sigma = 50$ system. The dashed continuations in this viewgraph correspond to average polymer concentration, average B compositions that are metastable. The extrapolated values for the polymer density indicated in the right ordinate are the densities expected for a polymer brush in the pure solvent B.

Let us finally discuss a system wherein both solvents are much better than the systems discussed above, $\chi_{PA} = 0$, $\chi_{PB} = -2$. In the box model this system was shown to have a continuous uptake of the wetting component B. Again a sparsely grafted brush $\sigma = 250$ is taken. In Figure 10 we present a family of adsorption isotherms in the region of the possible collapse phase transition where we have introduced the affinity for the wetting component with the surface as a new variable: $\chi_{BS} = 0, -1, -2, -3, -4, -5$ as indicated. The interactions of the solvent A and the polymer P with the surface remained athermal. In passing, we mention that in the box model this type of interactions is usually ignored. As could be expected, the family of isotherms clearly shows that it is possible to influence the prewetting behavior by this parameter. Also the range of parameters needed for these changes are small and experimentally accessible. There is a prewetting critical point in this system which is found close to $\chi_{BS} = -4$. For stronger affinities for B for the surface, the adsorption isotherms are smooth, showing no singularities. For weaker adsorption than $\chi_{BS} = -4$, a prewetting step is found, which becomes more pronounced when the substrate does not attract (or even repels) the B solvent. An important conclusion from Figure 10 is that in a rigorous analysis the effects of the wall should be included. This is especially important for the present systems, as the prewetting step is restricted to rather thin films near the surface.

In the inset of Figure 10, a larger part of a representative isotherm is shown. This isotherm shows that when $\chi_{PA} = 0$ and $\chi_{PB} = -2$, there is again a limit to the amount of solvent that can be absorbed into the brush. This amount appears to be independent of the strength by which the wetting solvent is attracted to the substrate. In other words, the amount of solvent trapped in the brush at coexistence is universal: it only depends on the brush characteristics and it is insensitive to the substrate properties. This agrees with earlier observations.[6,18]

4. Some Implications. The systems discussed above were shown to trap at coexistence a large, yet finite, amount of solvent in the brush: the systems were in fact very close to the wetting transition. Indeed in the box analysis it was (erroneously) judged that these systems were wet, i.e., that there were no limits to the film thickness at coexistence. The numerical SCF analysis captured an interesting mechanism to arrest the growth of the wetting film just below the wetting transition. This mechanism involves the possibility that some chains stretch beyond the already strongly stretched state in the brush to reach for the liquid−liquid interface. The fact that it is possible to trap a large amount of solvent into a brush is of course of special interest. Control over the thickness of the trapped film thickness may become of use to design colloidal systems with a tuneable outer layer with, e.g., special solubility characteristics. Experimental verification of the above findings may not necessarily be very complicated, as it is now possible to routinely and reproducibly make polymer brushes with controllable characteristics in the laboratory.

Conclusions

Numerical calculations in the self-consistent-field (SCF) approximation were used to describe the uptake of a minority solvent into a polymer brush from an binary mixture of solvents which have a solubility gap, which allows to test the results obtained before with a boxlike Alexander−de Gennes model. We have identified a number of important advantages of doing the full numerical analysis: (a) information about the density profiles of the polymer and of the solvent components as well as the distribution of the polymer chain ends is obtained, (b) the numerical model can account for adsorption effects both at the substrate and at the liquid−liquid interface, and (c) the numerical analysis is more powerful in discriminating between wetting and partial wetting. Nevertheless, the simple box model captures the physically important features of the system

and provides relatively simple relations. It is thus very helpful to identify the relevant and interesting parts of parameter space. Because of the large number of parameters in this system the box model has a real added value.

It is noteworthy that not only in the box model are approximations made. Also in the numerical SCF analysis the homogeneity of the system is overestimated since the lattice layers parallel to the grafting surface are considered as homogeneous. In principle, this could be remedied by using more time-consuming 2D SCF calculations.[17]

Both the box model and the SCF model show that the wetting of a polymer brush is of an extraordinary richness. It behaves nonclassically in several ways. From a wetting point of view it is a remarkable system because we may have cases that there is a prewetting step while the system (substrate plus brush) is not wet at coexistence (partial wetting). It is also nontrivial from a polymer-phase-transition point of view. Usually a polymer will swell with increasing solvent quality. In the present system, however, the transition is anomalous: the polymer collapses into the better solvent.

Finally, we mention that wetting transitions in polymer brushes should be relatively easily measurable and typically the wetting transitions are expected to be second order. This is noteworthy because at present there is just one experimental system reported in the literature with a second-order wetting transition:[19] in most cases one finds first-order wetting transitions.

Acknowledgment. This work was partially supported by the NOW Dutch−Russian program for Agricultural and Food Research and P/E in Complex Fluids and Gr. RFBR 99-03-33319.

References and Notes

(1) Milner, S. T. *Science* **1991**, *251*, 905.
(2) Milner, S. T.; Witten, T. A.; Cates, M. E. *Macromolecules* **1988**, *21*, 2610.
(3) Zhulina, E. B.; Pryamitsyn, V. A.; Borisov, O. V. *Polym. Sci. USSR* **1989**, *31*, 205.
(4) Wijmans, C. M.; Scheutjens, J. M. H. M.; Zhulina, E. B. *Macromolecules* **1992**, *25*, 2657.
(5) De Gennes, P.-G. *C. R. Acad. Sci. Paris, Ser. II* **1996**, *322*, 819.
(6) Leermakers, F. A. M.; Mercurieva, A. A.; van Male, J.; Zhulina, E. B.; Besseling, N. A. M.; Birshtein, T. M. *Langmuir*, submitted for publication.
(7) Lyatskaya Yu; Balazs, A. *Macromolecules* **1997**, *30*, 7588.
(8) Birshtein, T. M.; Zhulina, E. B.; Mercurieva, A. A. *Macromol. Theory Simul.*, submitted for publication.
(9) De Gennes, P.-G. *Macromolecules* **1980**, *13*, 1069.
(10) Alexander, S. *J. Phys.* **1977**, *38*, 983.
(11) Schick, M. *Liquids at Interfaces*; Charvolin, J., Joanny, J. F., Zinn-Justin, J., Eds.; North Holland: Amsterdam, 1990.
(12) Edwards, S. F. *Proc. Phys. Soc.* **1965**, *85*, 613.
(13) Fleer, G. J.; Cohen Stuart, M. A.; Scheutjens, J. M. H. M.; Cosgrove, T.; Vincent, B. *Polymers at Interfaces*; Chapman and Hall: London, 1993.
(14) Evers, O. A.; Scheutjens, J. M. H. M.; Fleer, G. J. *Macromolecules* **1990**, *23*, 5221.
(15) Amoskov, V. M.; Birshtein, T. M.; Pryamitsyn, V. A. *Macromolecules* **1996**, *29*, 7240.
(16) Birshtein, T. M.; Amoskov, V. M.; Mercurieva, A. A.; Pryamtisyn, V. A. *Macromol. Symp.* **1997**, *113*, 151.
(17) Schlangen, L. J. M.; Leermakers, F. A. M.; Koopal, L. K. *J. Chem. Soc., Faraday Trans.* **1996**, *92*, 579.
(18) Johner, A.; Marquess, C. M. *Phys. Rev. Lett.* **1992**, *69*, 1827.
(19) Ragil, K.; Meurnier, J.; Broseta, D.; Indekeu, J. O.; Bonn, D. *Phys. Rev. Lett.* **1996**, *77*, 1532 1996.

MA9910888